Journal of Thermal Analysis, Vol. 40 (1993) 915-922

STUDIES OF INFILTRATION BY APPARENT THERMOGRAVIMETRY

K. R. Lilius, M. M. Gasik, V. P. Järvelä and S. Strömberg

HELSINKI UNIVERSITY OF TECHNOLOGY, SF-02150 ESPOO 15, FINLAND

A technique named 'apparent thermogravimetry' (ATG) has been developed for studying infiltration phenomena. It has been used for investigating of infiltration of copper, cast iron, and cobalt alloys into porous tungsten, sintered steel, and tungsten carbide. A description of ATG signal behaviour has been obtained, taking into account 'internal' (capillary, viscous, gravitational, end-drag) and 'external' (wetting, buoyancy, Archimedean) forces. Dependencies of Archimedean force and wetting angle on different parameters are described in relation to the infiltration mechanism. The ATG method can be used to determine surface tension or contact angle.

Keywords: apparent thermogravimetry, infiltration phenomena

Introduction

The wettability of a solid by a liquid is important in many fields of science and technology. This paper describes the development of a special new thermoanalytical technique and its use in investigating infiltration processes taking place in processing metal and ceramic matrix composites. There are several methods for studying wetting and infiltration phenomena. These include sessile drop [1] and capillary rise methods [2]. Each has benefits and disadvantages. They are suitable for equilibrium wetting angle determination despite considerable inaccuracy in measurement [2, 3]. They cannot be used for infiltration kinetics investigations, where a specimen is intruded into a melt. This is the reason why a special theoretical background and measuring technique has been developed to obtain quantitative and qualitative description of infiltration processes. This method is termed 'apparent thermogravimetry' (ATG), and was developed at Helsinki University of Technology. Numerous measurements carried out on the W-Cu system are described here. From a theoretical basis, variables have been introduced to enable a quantitative description of infiltration processes. The results are con-

John Wiley & Sons, Limited, Chichester
Akadémiai Kiadó, Budapest

sidered to be in satisfactory agreement with the theory deduced, and are discussed in relation to known data [2, 4, 5].

Theoretical background

The equilibrium of the 'gas-liquid-solid' system can be expressed by Young's equation:

$$\gamma_{(l-g)}\cos\theta = \gamma_{(s-g)} - \gamma_{(s-l)}$$

where $\gamma_{(i-j)}$ represents the surface tension of the i–j interface, and θ is the contact angle [1, 2].

Klang [6] has reported the results of wettability measurements using TG (up to 800°C). The crucible with a melt was raised at a constant rate until the specimen was submerged in the melt; it was then held for more than 50 sec and then lowered. The weight of a specimen was measured continuously as in conventional TG methods, but in this case an 'apparent' TG-signal (ATG) in units of force (mN) was recorded. Taking into account all the forces in the process (gravity, Archimedean, buoyancy, and wetting), it is possible to deduce the dependence of the shape of an ATG-curve and the dynamics of a wetting process. However, this method can not be directly applied to infiltration measurements, because too many processes take place simultaneously and can not be distinguished. Good theoretical bases for infiltration have been presented [4, 7–9], but these are not compatible with thermogravimetric measurements. It is because of this that a general description of an ATG signal behaviour has to be deduced.

The porous body can be represented by a capillary tube [4] in which movement of the infiltrate is described as follows:

$$\vec{F_\gamma} + \vec{F_g} + \vec{F_\eta} + \vec{F_e} = \frac{\pi r^2}{\rho}\frac{d}{dt}(h\frac{dh}{dt})^2 \tag{1}$$

where F_i correspond to surface tension, gravitational, viscosity, and end-drag forces respectively, ρ is the infiltrate density, r is the radius of the capillary tube, and h is the position of the meniscus of the liquid in the tube, measured with respect to the surface of the liquid in the bath [4]:

$$\vec{F_\gamma} = 2\pi r\gamma\cos\theta\,; \quad \vec{F_g} = -\pi r^2\rho g h\,;$$

$$\vec{F_\eta} = -8\pi\eta h\frac{dh}{dt}\,; \quad \vec{F_e} = -\frac{\pi r^2\rho}{4}\left(\frac{dh}{dt}\right)^2.$$

However, the position of the surface of the melt depends on immersion depth (y) and infiltration rate at the time. The ATG signal will therefore be related to the vector sum of the forces applied to the specimen:

$$y\frac{d^2y}{dt^2}+\left(\frac{dy}{dt}\right)^2+gy-\frac{4gr^2}{\alpha d_s}(h+y)=\left(H_s\rho_s g+\frac{4\gamma\cos\theta}{\alpha d_s}\right)/\rho \qquad (2)$$

where g is the acceleration due to gravity, H_s, d_s, ρ_s are the height, diameter, and true density of the specimen, α is the fractional density of the specimen, and y is the 'liquid-vapour' surface tension. Furthermore, the infiltration velocity (dh/dt) is assumed to be connected to the rate of change of immersion depth (dy/dt) such that:

$$\frac{dh}{dt}=-\frac{D^2-d_s^2}{4r^2}\frac{dy}{dt} \qquad (3)$$

In this equation D represents the internal diameter of the crucible. This model allows a mathematical description of infiltration kinetics in the thermal balance setup.

Experimental

The thermobalance incorporates a tubular furnace with SiC heater (up to 1500°C) and lifting system for an alumina crucible containing the alloy (Fig. 1). The balance is based on a 'Mettler H 20E' system with electronic amplifier and strip-chart or XY-recorder. Temperature is controlled by Pt-Pt-10%Rh thermocouples. Platinum wire was also used for checking whether contact between specimen and alloy was achieved. Partial oxygen pressure was determined by an electrolytic ZrO_2-CaO cell. The crucible is raised at a constant rate until contact is made with the specimen, and then raised sharply to obtain the chosen immersion depth. This leads to a jump in the ATG signal, which is recorded simultaneously with temperature and oxygen potential of the gas phase.

The following materials were investigated: tungsten powders HC250/500 (mark B), its mix with 1% chromium (mark C), WA60 (mark D), W-DC (mark A), average particle size 2.5/5, 6.8, and 16 μm respectively; pure copper (alloy 1), and alloys Cu-10%Ag (2) and Cu-30%Ag (3). Specimens were mixed with binder, compacted to a desired density (about 60% T.D.), and sintered by different routes.

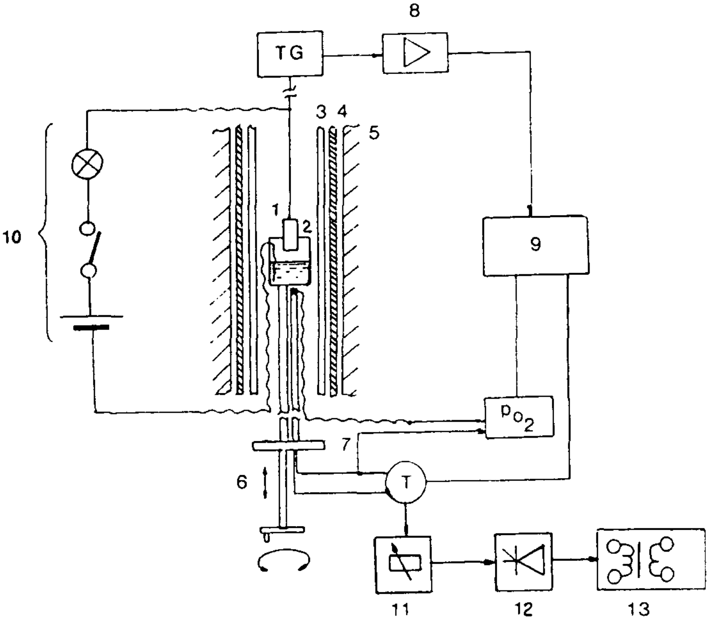

Fig. 1 Thermobalance system for infiltration: 1 - specimen, 2 - crucible with a melt, 3 - alumina tube, 4 - SiC heating element, 5 - furnace insulation, 6 - lifting/supporting system, 7 - Pt/PtRh thermocouples, 8 - amplifier, 9 - recorder, 10 - contact checking system, 11 - temperature control, 12 - thyristor unit, 13 - power supply

Results and discussion

Figure 2 gives an example of an ATG curve for the W-Cu system (specimen D, alloy 1, i.e. D-1), in which one can see different stages of infiltration. Because all the forces, which contribute to the ATG signal are in equilibrium at a particular time, the expression

$$\frac{8\gamma\cos\Theta}{5r}=\left(\frac{D^2-d_s^2}{4r^2}\right)^2\left(H_s\rho_s d+\frac{4\gamma\cos\theta}{\alpha d_s}\right) \tag{4}$$

leads to an estimate of $r = 91$ μm. The calculated initial infiltration rate $(\mathrm{d}h/\mathrm{d}t)_0$ equals 3.3 cm/sec, and the rate of change of immersion depth $(\mathrm{d}y/\mathrm{d}t)_0 = -2$ μm/sec. The next step is the determination of the Archimedean force:

$$\vec{F}_{\mathrm{Arc}}=-\frac{\pi d_s^2}{4}g\rho y+\pi d_s\gamma\cos\Theta \tag{5}$$

which has two main contributions, Archimedean buoyancy and surface interaction. For the final immersion depth $y = 1$ mm, it has been estimated that $F_{\mathrm{Arc}} = -3.9$ mN (measured from ATG signal $F_{\mathrm{Arc}} = -3.7$ mN). In this case the total weight force change equals 27.5 mN (i.e. the Archimedean force is approximately 14% of the apparent force due to increase in sample mass).

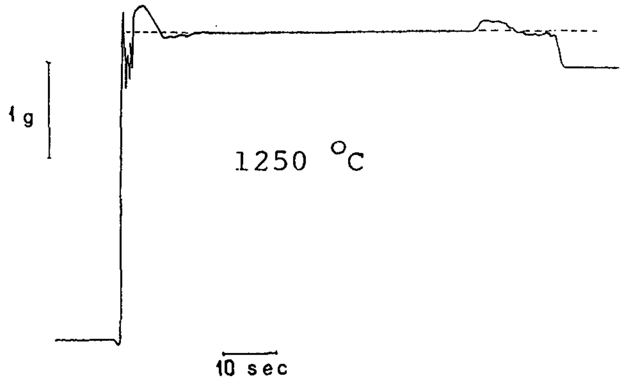

Fig. 2 Real time scale of infiltration measurements by the ATG method: porous tungsten, pure copper melt, hydrogen environment

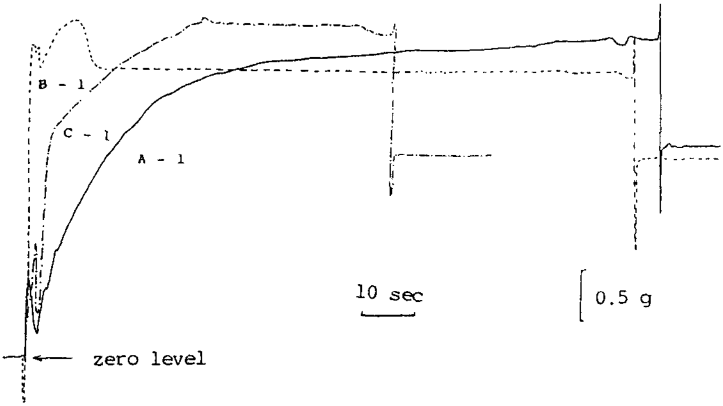

Fig. 3 ATG curves of pure copper infiltration in different tungsten samples

Results of these measurements are shown in Fig. 3. The infiltration rate (R_{I}), which is proportional to the first derivative of weight gain:

$$R_{\mathrm{I}}=\frac{d}{\mathrm{d}t}\left[\sum_{\mathrm{i}}\vec{F_{\mathrm{i}}}+\sum_{\mathrm{i}}\vec{P_{\mathrm{j}}}\right] \tag{6}$$

is higher for B than for C or A samples (alloy 1). Here F_{i} and P_{j} are forces applied inside capillaries and to the bulk specimen, respectively. If the radius of a model capillary tube (directly determined by average particle size [10]) decreases by about three times (A → B), it leads to an increase in R_{I} of 3 to 9 times depending which particular contribution is more important at the time. Because there are two phases with different densities, use of a formula based on a total weight gain is suggested. If all other parameters are equal, then one should consider the initial density of the specimen (ρ_{o}), density of W (ρ_{W}) and of an alloy (ρ_{A}), and final weight gain ($G = (m_{\mathrm{l}} - m_{\mathrm{o}}) / m_{\mathrm{o}}$). Thus the infiltration efficiency (IE) can be estimated from

$$IE=\frac{((1+G)^2-(\rho_{\mathrm{W}}+G\cdot\rho_{\mathrm{A}})/\rho_{\mathrm{W}})\rho_{\mathrm{o}}}{(\rho_{\mathrm{W}}+G\cdot\rho_{\mathrm{A}})(1-\rho_{\mathrm{o}}/\rho_{\mathrm{W}})}\cdot 100\% \tag{7}$$

and maximum weight gain $G_{\max}$ (corresponding to full infiltration $IE = 1$) from:

$$G_{\max}=\frac{\rho_{\mathrm{A}}}{\rho_{\mathrm{W}}}-\frac{\rho_{\mathrm{A}}}{2\rho_{\mathrm{o}}}-1+\frac{1}{2}\sqrt{\left(\frac{\rho_{\mathrm{A}}}{\rho_{\mathrm{o}}}+2\left(1-\frac{\rho_{\mathrm{A}}}{\rho_{\mathrm{W}}}\right)\right)^2-4\left(1-\frac{\rho_{\mathrm{W}}}{\rho_{\mathrm{o}}}\right)} \tag{8}$$

where $G_{\max}$ represents the theoretically possible amount of infiltrated alloy with a given density.

Proceeding to the next case (specimens B in various alloys), no significant difference has been obtained in the shapes of kinetic curves [10]. However on further comparison (various samples in alloy 2) results are seen to be clearly distinguished [10]. The R_{I} for A and B specimens appear similar, but are lower for case C.

Table 1 Infiltration efficiency IE and its dependence on alloy composition

Infiltration efficiency IE/%	Specimens		
	A	B	C
Alloy 1 (1120°C)	56.7	60.9	56.6
Alloy 2 (1080°C)	64.7	60.5	55.6
Alloy 3 (1030°C)	69.3*	63.4	52.3
Approximate equation (IE≈)	58.3+0.4%Ag	60.2+0.13%Ag	56.8–0.15%Ag

*for 1080°C

The infiltration efficiency *IE* for these measurements could be presented as follows (Table 1). For specimen B-3 there is no significant differences compared to B-1 and B-2.

However, the most significant result is an increase in ATG following removal of the specimen from the melt. This phenomenon has been reported to occur only under conditions when the Archimedean buoyancy exceeds surface interaction within the resulting force (5). This force is considered to be determined by both silver and chromium influences: $F_{\mathrm{Arc}} = f\,(\%\mathrm{Ag}, \%\mathrm{Cr})$. The data plot on a straight line for C samples ($F^{\mathrm{C}}_{\mathrm{Arc}} = 12.68 - 0.772\ \%\mathrm{Ag}$, mN), but these are no correlations for A and B. For immersion depth $y = 1$ mm, using Eq. (5) and known data for surface tension, one can estimate the apparent wetting angle for samples C as 74°, 88°, and 125° for alloys 1, 2 and 3, respectively. This also enables estimations of an 'equilibrium' contact angle by simple extrapolation of the difference in ATG signal values of final (immersed) weight and initial weight of the sample

$$\Delta = \pi d_{\mathrm{s}} \left(\frac{\gamma}{g} \cos\Theta - \frac{d_{\mathrm{s}}}{4} y\rho \right) \tag{9}$$

on zero immersion depth y. It gives 66° for pure copper, 80° for Cu-10%Ag, and 115° for Cu-30%Ag alloy. The first value is in satisfactory agreement with one (70°) reported earlier [10] for 1120°C. Therefore addition of silver to a copper melt makes wetting in the W-Cr system worse. To reveal the influence of Cr and Ag, the infiltration efficiency *IE* was calculated by Eq. (7). It also leads to the worst infiltration (Table 1) for the C-3 case (*IE* = 52% only) in comparison with both C-1 (57%) and B-1, 2 (60%).

The above discussion provides deeper insight into the infiltration mechanism. There is a very important phenomenon in the wetting of a clean metal surface by an alloy which is closely associated with the formation of a precursor film ahead of the bulk microscopic front of the liquid [11]. This has also been referred to a 'hysteresis of the wetting angle'. In such studies [11] microdrops clearly indicating condensation of the infiltrant metal vapour have been revealed, so adsorption of vapour can take place rapidly ahead by either vapour migration or evaporation-condensation process. Based on these observations the following mechanism of infiltration is suggested.

Either copper (silver) vapour or both are chemically adsorbed on the tungsten surface. This leads to increased ease of physical adsorption of the next thin layer and its condensation. After a critical thickness of the precursor film is reached, the influence of surface electronic states of tungsten on atoms of a metal will disappear, i.e. this will be the moment when 'melt-on-melt' spreading will take place with $\cos\Theta = 0$ and the development of a coherent interface. The spreading of a melt leads to reaction interface advance, which in its turn produces renewal of the precursor film.

We consider that this method is capable of determining both surface tension and contact angles. However, more theoretical background still needs to be developed, especially for complicated systems where one has to take account of mutual solubility and interaction between liquid and solid phase.

Conclusions

The apparent thermogravimetry (ATG) method has been described together with theoretical background, and has been confirmed experimentally for the W-Cu system. This technique shows promise not only for infiltration studies but also for unknown wetting angle determinations.

References

1 U. Bröckel and F. Löffler, Part. and Part. Syst. Charact., 8 (1991) 215.
2 P. R. Chidambaram, G. R. Edwards and D. L. Olson, Met. Trans., 23B (1992) 215.
3 K. C. Russel, J. A. Cornie and S. Y. Oh, Proc. Symp. Ann. Meet. Metal. Soc. AIME, Warrendale, PA; USA 1986, pp. 61–91.
4 G. P. Martins, D. L. Olson and G. R. Edwards, Met. Trans., 19B (1988) 95.
5 J. Senkara and W. K. Wlosinski, J. Mater. Sci., 20 (1985) 3597.
6 L-G. Klang, Report IM-2674, Swedish Institute for Metals Research, Stockholm 1991.
7 A. Mortensen, L. J. Masur, J. A. Cornie et al., Met. Trans., 20A (1989) 2535.
8 A. Mortensen and V. Michaud, Metal. Trans., 21A (1990) 2059.
9 S. Nourbakhsh, F.-L. Liang and H. Margolin, Metal. Trans., 20A (1989) 1861.
10 S. Kolu and V. Järvelä, Literature survey report. Helsinki University of Technology, 1991.
11 J. H. Ahn and A. Berghezan, Mater. Sci. Technol., 7 (1991) 643.

Zusammenfassung — Zur Untersuchung von Infiltrationserscheinungen wurde eine Technik mit dem Namen "Scheinthermogravimetrie" (ATG) entwickelt. Sie wurde zur Untersuchung des Eindringens von Kupfer, Gußeisen und Kobaltlegierungen in porösem Wolfram, Sinterstahl und Wolframcarbid verwendet. Unter Berücksichtigung von "internen" (Kapillar-, Viskose-, Gravitations- und Endwiderstands-) und "externen" (Benetzungs-, hydrostatischen Auftriebs- und Archimedes'schen) Kräften konnte man eine das ATG-Signal-Verhalten beschreiben. Im Hinblick auf den Infiltrationsmechanismus wurde die Abhängigkeit von Archimedes'schen Kräften und Benetzungswinkeln von verschiedenen Parametern diskutiert. Die ATG Methode kann zur Bestimmung von Oberflächendampfdruck und Benetzungswinkel eingesetzt werden.